https://doi.org/10.5194/gmd-2024-158
Preprint. Discussion started: 25 September 2024

Geoscientific Model Development Discussions
Open Access

Estimation of above- and below-ground ecosystem parameters for the DVM-DOS-TEM v0.7.0 model using MADS v1.7.3: a synthetic case study

Elchin E. Jafarov[1], Hélène Genet[2], Velimir V. Vesselinov (Monty)[3], Valeria Briones[1], Aiza Kabeer[4], Andrew L. Mullen[1], Benjamin Maglio[2], Tobey Carman[2], Ruth Rutter[2], Joy Clein[2], Chu-Chun Chang[1], Dogukan Teber[1], Trevor Smith[1], Joshua M. Rady[1], Christina Schädel[1], Jennifer D. Watts[1], Brendan M. Rogers[1], Susan M. Natali[1]

[1]Woodwell Climate Research Center, Falmouth, MA, USA
[2]Institute of Arctic Biology, University of Alaska Fairbanks, Fairbanks, AK, USA
[3]EnviTrace LLC, NM, USA
[4]Program in Applied Mathematics, University of Arizona, Tucson, AZ, USA

Correspondence to: Elchin E. Jafarov (ejafarov@woodwellclimate.org)

Abstract.
The permafrost region contains a significant portion of the world's soil organic carbon, and its thawing, driven by accelerated Arctic warming, could lead to the substantial release of greenhouse gases, potentially disrupting the global climate system. Accurate predictions of carbon cycling in permafrost ecosystems hinge on the robust calibration of model parameters. However, manually calibrating numerous parameters in complex process-based models is labor-intensive and further complicated by equifinality - the presence of multiple parameter sets that can equally fit the observed data. Incorrect calibration can lead to unrealistic ecological predictions. In this study, we employed the Model Analysis and Decision Support (MADS) software package to automate and enhance the accuracy of parameter calibration for carbon dynamics within the coupled Dynamic Vegetation Model, Dynamic Organic Soil Model, and Terrestrial Ecosystem Model (DVM-DOS-TEM), a process-based ecosystem model designed for high-latitude regions. The calibration process involved adjusting rate-limiting parameters to accurately replicate observed carbon and nitrogen fluxes and stocks in both soil and vegetation. Gross primary production, net primary production, vegetation carbon, vegetation nitrogen, and soil carbon and nitrogen pools served as synthetic observations for a black spruce boreal forest ecosystem. To validate the efficiency of this new calibration method, we utilized model-generated synthetic observations. This study demonstrates the calibration workflow, offers an in-depth analysis of the relationships between parameters and synthetic observations, and evaluates the accuracy of the calibrated parameter values.

https://doi.org/10.5194/gmd-2024-158
Preprint. Discussion started: 25 September 2024

1 Introduction

The permafrost region contains 1,440-1,600 petagrams of organic carbon in its soils, representing nearly half of the world's soil organic carbon pool (Hugelius et al., 2014; Schuur et al., 2022). Accelerated warming in the Arctic leads to permafrost thaw, resulting in the decomposition and potential release of a substantial portion of this stored carbon as greenhouse gases, significantly impacting the global climate system (Natali et al., 2021; Schuur et al., 2022; Treharne et al., 2022). The permafrost carbon-climate feedback remains one of the largest sources of model uncertainty for future climate predictions, as critical ecological and biogeochemical processes are poorly represented and constrained in ecosystem models, if included at all (McGuire et al., 2016, 2018; Schädel et al., 2024). To predict future permafrost evolution, models rely on various parameters that contribute to a wide uncertainty range in predictions of permafrost warming (Andresen et al., 2020; Harp et al., 2016; Schädel et al., 2024). Thus, the development of parameter calibration methods is an essential step toward improving prediction accuracy and deepening our understanding of permafrost dynamics and future permafrost carbon-climate feedbacks.

Calibration involves estimating and adjusting model parameters and constants to enhance the agreement between model outputs and observed data, with the model serving as a mathematical representation of ecological and physical processes (Rykiel, 1996). These parameters are often rate or transport constants that are onerous or impractical to empirically estimate, though model outputs can be highly sensitive to them. Since many model representations are grounded in physics, generalized physical laws are often used to describe ecological and cryohydrological processes. Typically, model outputs are validated against data from laboratory experiments, idealized mathematical models, or site-specific observations, also referred to as target data. During this validation, model parameters are adjusted so that model outputs match the target data. The validated model is then applied to broader geographic locations and/or different time periods, assuming that the validation data represent the environment or ecosystem for which the parameters were calibrated.

Parameter calibration for complex process-based models is often constrained by the significant labor required and the limited availability of sites with the necessary observations, especially in permafrost regions. Despite these challenges, process-based models remain essential because they encapsulate our current understanding of ecosystem functions and structures, serving as powerful tools for extrapolation. The assumption of representativeness is intrinsic to these models, as they are designed to simulate processes that reflect our best understanding of ecosystem dynamics, allowing for their application beyond the specific sites where they have been initially parameterized. The approach of extrapolating model parameterization for ecosystems of the same type, across wider regions is standard and widely used within ecosystem modeling communities (McGuire et al., 2018; Matthes et al., 2024). Additionally, the role of ecosystem diversity on the spatio-temporal patterns of ecosystem carbon dynamics in the permafrost region has been characterized by numerous empirical studies (Euskirchen et al., 2014; Melvin et al., 2015) and evaluated by modeling investigations (Lara et al., 2016). Therefore, a critical step in improving model accuracy involves calibrating the model against data for a representative diversity of ecosystem types in the Arctic

https://doi.org/10.5194/gmd-2024-158
Preprint. Discussion started: 25 September 2024

Geoscientific Model Development Discussions

where observations are available. To prepare an ecosystem model for this extensive calibration task, it is essential to develop robust calibration tools and methods that can automate the process of efficiently optimizing model parameters.

Another well-known and significant issue in optimizing model parameters through calibration, also referred to as parameter estimation or optimization, is the existence of equifinality (Jafarov et al., 2020; Nicolsky et al., 2007; Tran et al., 2017). Parameterization equifinality occurs when different sets of parameter values result in the same or similar model predictions, given that the model, forcing data, and observations used in calibration are the same (Beven and Freer, 2001). Model equifinality can subsequently lead to different outcomes in model projections. Multiple random initial guesses are used to address this challenge. If the majority of calibration tests with different initial guesses yield a good fit with observations and result in optimal parameter sets that are similar or closely aligned, it increases confidence that the recovered parameter set is indeed optimal. This approach mitigates the risk of converging on a local minimum and ensures a more robust and reliable parameter estimation process (Hansen, 1998).

Various methods have been employed to improve the calibration of model parameters across multiple scientific disciplines, utilizing sophisticated techniques and integrating diverse data sources such as remote sensing and field measurements, while accounting for model and data uncertainty (Dietze et al., 2018; Efstratiadis and Koutsoyiannis, 2010; Luo et al., 2016). Optimization-based inverse methods have been successfully used to calibrate parameters in physical models, including snow properties and subsurface thermo-hydrological properties (Jafarov et al., 2014, 2020), as well as soil properties for permafrost modeling (Nicolsky et al., 2007, 2009). However, inverse modeling can become computationally intractable when applied to complex process-based models (Linde et al., 2015).

Markov Chain Monte Carlo (MCMC) and data assimilation (DA) techniques have been employed to optimize model parameters by synchronizing model outputs with observed data, thereby enhancing model prediction accuracy (Brunetti et al., 2023; Fer et al., 2018; Xu et al., 2017). These methods often leverage Bayesian inference to address structural uncertainties within models. Nonetheless, the computational demand required for conducting MCMC simulations can outweigh the gains in model accuracy, particularly when dealing with complex process-based models with slow turnover rates that necessitate long simulations to reach equilibrium.

In recent years, DA techniques have been applied to optimize both model state variables (Fox et al., 2018; Ling et al., 2019) and parameters (Bloom et al., 2016; Peylin et al., 2016; Scholze et al., 2016; Schürmann et al., 2016). However, DA also encounters challenges related to unbalanced outputs and the need for extended simulations to achieve equilibrium. Persistent issues include the incorrect characterization of the error covariance matrix, which can lead to inaccurate posterior parameter values due to unaccounted model structural errors and observation biases (MacBean et al., 2016; Wutzler and Carvalhais, 2014).

Geoscientific Model Development
Discussions

Various surrogate-based optimization approaches have been proposed to alleviate the computational burden associated with parameter calibration (Koziel et al., 2011; Queipo et al., 2005). Surrogate models, also known as reduced-order models, simplify certain physical processes to approximate the underlying dynamics of the real model while being computationally less demanding (Forrester et al., 2006). By simplifying specific aspects of the model, surrogate models retain essential characteristics of the original system, allowing for faster and more efficient calibration without significantly compromising accuracy (Razavi et al., 2012; Regis and Shoemaker, 2007). However, simplifying complex models presents significant challenges. It is often unclear which assumptions can be safely made and which should be avoided, potentially leading to a loss of model accuracy. Surrogate models must carefully balance the trade-off between simplification and the retention of critical model characteristics to ensure reliable performance. This complexity necessitates rigorous validation to confirm that the surrogate model provides an adequate approximation of the real system without introducing significant errors.

In recent years, machine learning-based emulators, often referred to as "models of models," have emerged as a promising approach to reduce the computational burden associated with parameter calibration in complex ecosystem models (Castelletti et al., 2012; Fer et al., 2018; Reichstein et al., 2019). These emulators aim to approximate the outputs of physical and process-based models by learning the relationships between model inputs and outputs through multi-dimensional matrices, significantly enhancing computational efficiency. Unlike traditional surrogate models, which simplify the physical processes within a model, emulators strive to mimic the full complexity of the original model while requiring less computational power. For instance, Dagon et al., (2020) utilized artificial neural networks to emulate the Community Land Model version 5 outputs, focusing on biophysical parameter estimation and global calibration. By integrating machine learning techniques, they were able to explore parameter spaces more efficiently and achieve better alignment with observed data. This method demonstrates the potential of machine learning emulators in improving the accuracy and efficiency of parameter calibration in ecosystem models, particularly when faced with the challenge of high computational demands.

To facilitate the automation of the calibration process while minimizing computational demand and avoiding the oversimplification of ecological processes and feedbacks, we employed a non-linear least squares approach for our calibration. We utilized the Model Analysis and Decision Support (MADS) software package (Barajas-Solano et al., 2015; O'Malley and Vesselinov, 2015) for parameter calibration of a terrestrial ecosystem permafrost-enabled model. MADS has been actively developed since 2010, and its conversion to the Julia programming language has provided automatic differentiation capabilities suitable for calibration problems, improving computational efficiency (Vesselinov V.V., 2022).

In this study, we developed an automated parameter calibration method for a process-based terrestrial ecosystem model developed for high-latitude regions and characterized by a high level of complexity. To demonstrate its efficacy, we utilized synthetic data and evaluated the capacity of the calibration method to recover the data after perturbing initial guesses (a given set of parameters) using random sampling. The model was run using known parameter values, and the resulting outputs were treated as observations. The primary objective was to illustrate that the parameter calibration method could recover the

https://doi.org/10.5194/gmd-2024-158
Preprint. Discussion started: 25 September 2024

synthetic parameter set successfully. The secondary objective was to optimize and reduce the labor and time associated with manual parameter calibration. We developed and tested our calibration method for the coupled dynamic vegetation model, dynamic organic soil, and terrestrial ecosystem model (DVM-DOS-TEM) and tested our approach using synthetic observations at a black spruce forest site, a dominant community type in Interior Alaska.

2 Methods

2.1 Synthetic data for Black Spruce Forest site

The two most common forest types in interior Alaska are evergreen stands of black spruce and mixed spruce-deciduous broadleaf forests. Approximately 39% of Interior Alaska is covered by evergreen forest stands and 24% by deciduous forest stands (Calef et al., 2005; Jean et al., 2020). In our study, we developed model calibration for a black spruce (*Picea mariana*) forest community type (CMT), using observations collected in a site located within the Tanana Valley State Forest, just outside Fairbanks, Alaska (64°53′N, 148°23′W). Carbon (C) and nitrogen (N) cycling and environmental monitoring in this forest stand were originally observed by Melvin et al., (2015). The Murphy Dome fire 1958, which covered 8,930 hectares, burned this area and resulted in complete stand mortality.

We used Gross Primary Productivity without N limitation (GPP*), Net Primary Productivity (NPP), Vegetation C, and Vegetation N stocks by compartments (i.e. roots, stems, and leaves) as synthetic observations shown in Table 1. Synthetic observations are model-generated data that simulate actual measurements using known parameter values, referred to as synthetic target values. To generate these target values, we used existing parameters and the setup described in Section 2.3. The target values shown in Table 1 represent the state of the ecosystem where vegetation and below-ground C stocks are in a steady state. Table 2 includes the below-ground target values. The model was previously manually calibrated using observations from the site. The actual observations were collected and prepared from the measured data at the site and from existing literature and published datasets. Data pre-processing was required before the time series data could be analyzed. Pre-processing was performed to identify and resolve missing data, inconsistencies, and potential outliers. In addition, site observations were aggregated to a monthly resolution to match the temporal resolution of the model outputs, and unit transformations were applied when needed to standardize the units of each variable. Target values for the site were compiled from various data literature sources containing information on C and N stocks, plant biomass, soil horizon depths, and productivity. However, following the initial calibration, the model outputs were similar but did not exactly match the target observations. As stated above, we choose synthetic targets because we know a set of parameters used to produce them and can compare how closely we can recover known parameter values. Therefore, we used the actual model output as our synthetic target values.

Table 1: Synthetic vegetation target values for the black spruce forest site used in the parameter calibration process

https://doi.org/10.5194/gmd-2024-158
Preprint. Discussion started: 25 September 2024

Above-ground Target Names	Notation	Units	Plant Functional Types			
			Evergreen Tree	Deciduous Shrub	Deciduous Tree	Moss
Gross Primary Productivity without nitrogen limitation	GPP^*	[gC/m^2/year]	307.17	24.53	46.53	54.23
Net Primary Productivity	NPP	[gC/m^2/year]	113.08	11.3	24.02	32.41
Vegetation Carbon Leaf	C_{leaf}	[gC/m^2]	572.36	8.35	6.14	136.54
Vegetation Carbon Stem	C_{stem}	[gC/m^2]	1894.03	98.90	477.80	
Vegetation Carbon Root	C_{root}	[gC/m^2]	474.55	33.19	7.17	
Vegetation Nitrogen Leaf	N_{leaf}	[gC/m^2]	14.79	0.38	0.57	1.15
Vegetation Nitrogen Stem	N_{stem}	[gC/m^2]	30.26	2.6	12.53	
Vegetation Nitrogen Root	N_{root}	[gC/m^2]	9.51	0.72	0.16	

Table 2: Synthetic below-ground target values for the black spruce forest site used in the parameter calibration process

Below-ground Targets Names	Notation	Unit	Value
Carbon Shallow	$C_{shallow}$	g/m2	888.91
Carbon Deep	C_{deep}	g/m2	3174.53
Carbon Mineral Sum	$\sum C_{mineral}$	g/m2	19821.50
Available Nitrogen Sum	$\sum N_{avail}$	g/m2	0.76

2.2 DVM-DOS-TEM description

DVM-DOS-TEM is a process-based biosphere model designed to simulate biophysical and biogeochemical processes between the soil, vegetation, and atmosphere. DVM-DOS-TEM has been applied extensively in Arctic and Boreal ecosystems in permafrost and non-permafrost regions (Briones et al., 2024; Euskirchen et al., 2022; Genet et al., 2013, 2018; Jafarov et al., 2013; Yi et al., 2009, 2010). This model focuses on representing C and N cycles in high-latitude ecosystems and how they are affected at seasonal (i.e., monthly) to centennial scales by climate, disturbances (Genet et al., 2013, 2018; Kelly et al., 2013), biophysical processes such as soil thermal and hydrological dynamics (McGuire et al., 2018; Yi et al., 2009; Zhuang et al., 2002), snow cover (Euskirchen et al., 2006), and plant canopy development (Euskirchen et al., 2014). Modeled vegetation is structured into multiple tiers: (1) the CMT represents the land cover class and characterizes vegetation composition and soil structure at the gridcell level (spatial unit, e.g. black spruce forest, tussock tundra, bog), (2) plant functional types (groups of species sharing similar ecological traits) characterize the vegetation composition within every CMT (e.g. black spruce forest community would be composed of evergreen trees, deciduous shrubs and sphagnum and feather moss plant functional types), and (3) plant structural compartments (leaves, stems, roots). The soil column is split into multiple horizons (fibric, humic, mineral, and rock/parent material). Every horizon is split into multiple layers for which C, N, temperature, and water content are simulated individually. The biophysical processes represented in DVM-DOS-TEM include radiation and water fluxes between the atmosphere, vegetation canopy, snow, and soil. Soil moisture and temperature are updated at a pseudo-daily time step (from linear interpolation of monthly climate forcings). A two-directional Stefan Algorithm is used to predict the positions of freezing/thawing fronts in the soil. The Richards equation is used to calculate soil moisture changes in the unfrozen layers of soil. Both the thermal and hydraulic properties of soil layers are affected by their water content (Yi et al., 2009, 2010; Zhuang et al., 2002). The ecological processes represented in DVM-DOS-TEM include C and N dynamics for every plant functional type of the vegetation community and every layer of the soil column. C and N dynamics are driven by climate, atmospheric chemistry, soil and canopy environment, and wildfire occurrence and severity. C and N cycles are coupled in the soil and the vegetation processes. The GPP of each plant function type is limited by N availability. When resources in N are limited, GPP is downregulated for all plant functional types (PFTs) based on a comparison of N demand (N required to build new tissues) and N supply in the ecosystem (Euskirchen et al., 2009). C and N from the litterfall are divided into aboveground and belowground. Aboveground litterfall is assigned only to the top layer of the soil column, while belowground litterfall (root mortality) is assigned to different layers of the three soil horizons based on the fractional distribution of fine roots with depth.

2.3 Input data used for equilibrium run

The driving inputs for the DVM-DOS-TEM model comprise spatial distribution of CMTs, landform, and mineral soil texture. These initialization data were forced to field observations at the study site (Melvin et al., 2015). The spatiotemporal dynamics of the model are driven by an annual time series of atmospheric CO_2 concentration (not spatially explicit), annual time series of spatially explicit distribution of fire scars and dates, and a spatially explicit monthly time series of climate, including mean air temperature, total precipitation, net incoming shortwave radiation, and vapor pressure (Genet et al., 2018). For the present study, we use historical climate data from 1901 to 2015, sourced from the Climatic Research Unit time series version 4.0 (CRU TS4.0; Harris et al., 2014) and downscaled at a 1-km resolution using the delta method (Pastick et al., 2017). For the

https://doi.org/10.5194/gmd-2024-158
Preprint. Discussion started: 25 September 2024

equilibrium run, the model was driven using the averaged climate forcings from the 1901-1930 period for the study site location, repeated continuously for a sufficient period so equilibrium of vegetation and below-ground C fluxes and stocks was achieved. The resulting modeled ecosystem state for each site then serves as the baseline for historical simulations, however, the calibration process described here only utilized outputs from the equilibrium.

2.4 MADS parameter calibration

We employed the Model Analysis and Decision Support (MADS) software package for parameter calibration of DVM-DOS-TEM, aiming to minimize the discrepancy between synthetic target and modeled data at the selected site (Barajas-Solano et al., 2015; O'Malley and Vesselinov, 2015). Since its inception in 2010, MADS has undergone active development, including a transition to the Julia programming language, which supports automatic differentiation suitable for calibration problems(Vesselinov V.V., 2022).

To set up the parameter calibration using the MADS package for the DVM-DOS-TEM model (Fig. 1), several components are required: the initial guess represents a set of parameter values to be passed to the DVM-DOS-TEM model; the target values; and a model function that updates the parameter file and executes the DVM-DOS-TEM model using the updated values. Parameter keys are used for parameter identification and tracking, and each parameter has a defined range, uniformly distributed within specified limits. Parameter range limits were determined based on prior knowledge. If certain observations are more critical than others, they can be weighted accordingly. For consistency of the calibration process for all parameters, we did not weight parameters in our setup (weight for all parameters were set to 1.0). The experiment name is used for bookkeeping purposes.

```
Md = Mads.create_problem(
     initial_guess,         #the set of initial values
     targets,               #the set of observations (targets)
     DVMDOSTEM_run,         #function that runs the model
     param_keys,            #list of parameter names
     param_distributions,   #the set of parameter ranges
     observations_count,    #number of observations
     observation_weights,   #the set of observation weights
     problem_name           #the name of the experiments
)
Mads.calibraterandom(md, 10; tolOF=0.01, tolOFcount=4)
```

Figure 1. The example of the Julia code setup using Model Analysis and Decision Support (MADS) functions.

In Figure 1, the `calibraterandom` function initiates the calibration process by randomly distributing parameter values within the specified ranges and then running the model calibration for the generated parameter sets. This function constructs

https://doi.org/10.5194/gmd-2024-158
Preprint. Discussion started: 25 September 2024

an objective function to minimize the difference between observed and modeled values (detailed in Section 2.5). The calculated residuals are used to assess method convergence. The calibration process employs a tolerance value for the objective function, denoted as `tolOF`, as the convergence criterion. The `tolOFcount` represents the number of iterations after which calibration ceases if the change in the objective function is minimal between iterations. While increasing the number of iterations could enhance calibration accuracy, it would also raise computational time. More information on the MADS functions can be found at the MADS website (https://madsjulia.github.io/Mads.jl)

2.5 MADS minimization method

The MADS package utilizes the Levenberg-Marquardt (LM) algorithm (Levenberg, 1944; Marquardt, 1963; Pujol, 2007) to minimize the difference (the sum of squared residuals) between observations and modeled predictions. In SI1, we provide more details on LM algorithm. The LM optimization method designed to solve non-linear least squares optimization/minimization problems, which are common in the field of history matching, model inversion, curve fitting, and parameter estimation. It combines two approaches: the first-order steepest-descent gradient method and the second-order Gauss-Newton method. This steepest-descent gradient method updates parameter values in the direction opposite to the gradient, thereby it is generally efficient in finding local minima. The Gauss-Newton method assumes that in a region close to the solution, the solved objective function behaves quadratically.

The algorithm begins by selecting an initial estimate for the parameters that need to be optimized (Fig S1). This initial guess is important as it sets the starting point for the optimization process. In our experiment, the initial guess is randomly generated from within the provided range near `true` parameter values. Alternatively, users can provide the initial guess. However, exploring a set of random initial guesses provides an efficient approach to exploring the parameter space and discrimination between local and global minima. In LM, we set the damping parameter (the Marquardt lambda) to 0.01. This parameter helps in adjusting the steps taken during the optimization process, balancing between the two optimization strategies (the first- and the second order techniques discussed above).

The main advantages of the LM method are its robustness and minimal computational demand. It effectively handles ill-conditioned problems where other optimization methods might fail (Lin et al., 2016; Pujol, 2007). Additionally, for problems well-suited to the Gauss-Newton method, LM often converges faster than gradient descent, making it an efficient choice for many non-linear least squares problems.

The disadvantage of the Levenberg-Marquardt (LM) method is its sensitivity to the initial parameter guesses. In addition, the compute speed deteriorates with the higher number of parameters used in calibration. It requires the computation of the Jacobian matrix and its pseudo-inverse, which can be computationally expensive for large-scale problems. Additionally, like many optimization methods, it can be sensitive to the initial parameter guess, potentially affecting its efficiency and convergence. In these cases, MADS provides alternative efficient approaches to address these computational challenges, such as (1) initializing the calibration with random initial guesses, (2) multiple restarts of the LM algorithms throughout the

https://doi.org/10.5194/gmd-2024-158
Preprint. Discussion started: 25 September 2024

minimization process, and (3) exploration of a series of alternative values for various parameters controlling LM performance (Lin et al., 2016).

2.6 Parameters and Calibration Targets

The calibration process in DVM-DOS-TEM is currently focused on the C and N annual cycles. Thus, calibrated parameters are associated with and adjusted to the major C and N fluxes and stocks in the vegetation and the soil. The calibration process follows a hierarchical approach (Figure 2), in which parameters to be calibrated are organized in hierarchical levels associated with (1) model complexity and feedback and (2) turnover of the processes the parameters are associated with. Therefore, parameters related to vegetation dynamics are calibrated first, followed by the slowest soil-related parameters.

The first step of the calibration relates to the simplest, fastest, first-order process in DVM-DOS-TEM, and consists of adjusting the rate limiting parameter of maximum C assimilation of the vegetation (c_{max}) driving vegetation GPP. Under baseline climate, the main limiting parameter of vegetation productivity in the Arctic is N availability (Chapin and Kedrowski, 1983) . Therefore, c_{max} is calibrated to reproduce estimates of GPP from fertilization experiments where N limitation is lifted. When fertilization experiments are not available for the community/region of interest, it is estimated by applying a multiplicative factor to observed GPP under natural conditions. This multiplicative factor is estimated from published fertilization experiments in similar communities and computed as the ratio between GPP estimated in fertilized plots and GPP estimated in control plots. Based on the literature, this fertilization factor can vary from 1.25 to 1.5 (Ruess et al., 1996; Shaver and Chapin, 1995).

The second step of the calibration process consists of turning on the representation of N limitation on vegetation productivity in the model (Euskirchen et al., 2009) and calibrating the rest of the vegetation-related parameters. In the current workflow, it consists of three substeps. These substeps could follow a different order based on the preference of the user and the specifics of a given site. These are rate-limiting parameters for maintenance respiration (Kr_b), maximum plant N uptake (n_{max}), C and N litterfall (c_{fall} and n_{fall} respectively). These parameters are adjusted until DVM-DOS-TEM outputs match observations of GPP and NPP, plant N uptake (Nup), and vegetation C and N pools, respectively). Target values of these variables are listed in Table 1. It is important to note that the parameters Kr_b, c_{fall}, and n_{fall}, as well as the variables for vegetation C and N, are specified per PFT and per compartment (leaf, stem, root).

In the third step, the rate-limiting parameters of soil heterotrophic respiration (kdc) and rate of microbial N uptake (n_{micb}^{up}) are calibrated as soil processes and takes longer to run in comparison to first two steps. These parameters are adjusted until DVM-DOS-TEM outputs match observations of soil organic C and available N stocks. Target values of these variables are listed in Table 2. In a final state, vegetation-related parameters are checked for a final adjustment after soil calibration, as soil processes can feedback to vegetation dynamics.

https://doi.org/10.5194/gmd-2024-158
Preprint. Discussion started: 25 September 2024

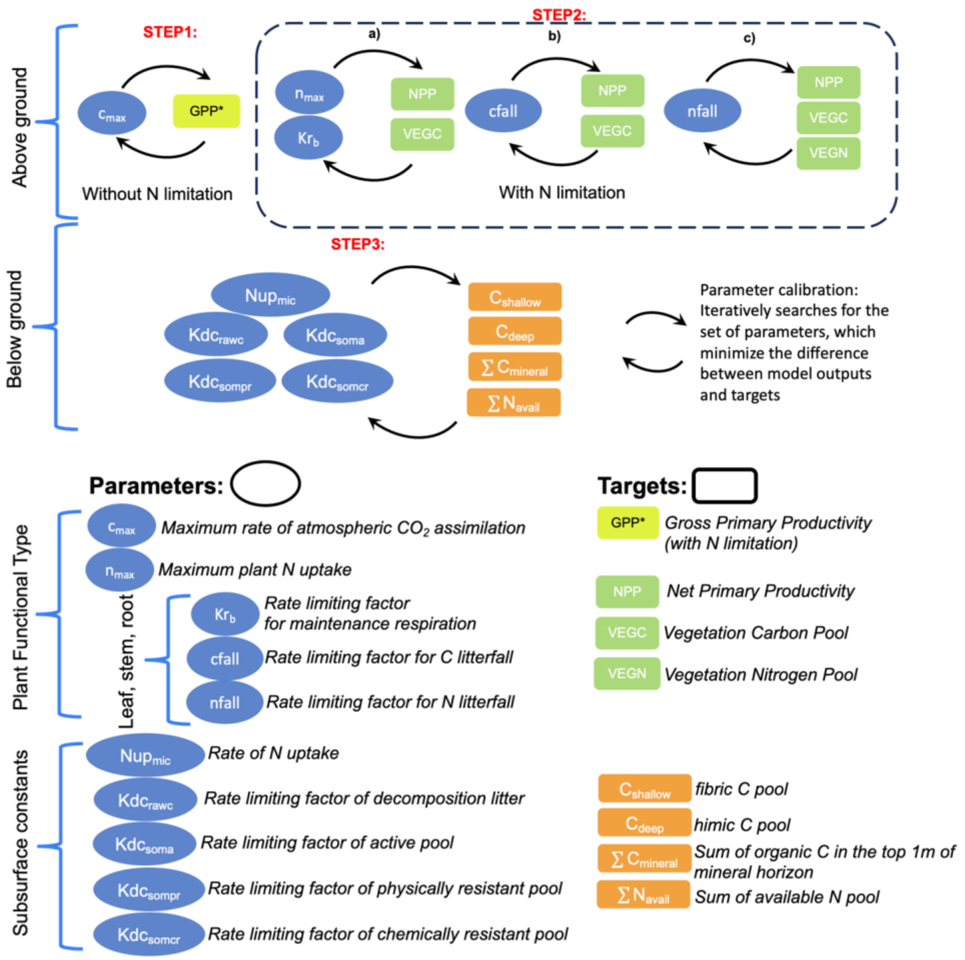

Figure 2. Schematics of the DVM-DOS-TEM model parameters and targets participated in the calibration process.

2.8 Calibrations setup and evaluation metric

Table 3 shows the parameter values used to calculate synthetic target values. We established four cases by perturbing the parameters by 10%, 20%, 50%, and 90% from their original values. For each case, the MADS `calibraterandom` function randomly sampled ten sets of parameters within the specified ranges (see Figure 1a). These ten sets of randomly perturbed parameters were then optimized using the MADS algorithm (Figure 1b). For each set of calibrated parameters and targets, we computed the root mean square error (RMSE) and relative error (RE) metrics. RMSE is employed to measure the magnitude of varying quantities, while RE gauges the absolute difference relative to the actual values. Given that some parameters are

https://doi.org/10.5194/gmd-2024-158
Preprint. Discussion started: 25 September 2024

small (less than 10^{-3}), the relative error provides more informative insights. The following equations were used to compute these metrics:

$$RMSE = \sqrt{(\overline{x} - x)^2}\,, \tag{1}$$

$$RE = \left|\frac{\overline{x}-x}{x}\right| \cdot 100\%, \tag{2}$$

where $\overline{x}$ is the mean of the best five out of ten computed target/parameter matches and x is a synthetic target value. To ensure the selection of the best-fitting parameters, we sorted error values from the lowest to the highest. Then, we selected the top five parameter sets, calculated their mean values, and compared these averaged parameters with the synthetic target values and known parameters.

Table 3: Synthetic parameter values for the black spruce forest site used in the parameter calibration process.

Name	Parameters	Units	Plant Functional Types			
			Evergreen Tree	Deciduous Shrub	Deciduous Tree	Moss
Maximum rate of atmospheric CO_2 assimilation	c_{max}	gC/m2/ month	381.19	113.93	210.48	93.31
Maximum rate of plant N uptake	n_{max}	gN/m^2/ month	3.38	1.55	1.0	3.55
rate limiting factor for C litterfall for leaf	c_{fall}^{leaf}	month^{-1}	0.0011	0.05	0.025	0.02
… for stem	c_{fall}^{stem}	month^{-1}	0.0034	0.0048	0.0036	
… for root	c_{fall}^{root}	month^{-1}	0.0052	0.0012	0.026	
Rate limiting factor for N litterfall for leaf	n_{fall}^{leaf}	month^{-1}	0.0102	0.045	0.018	0.007
… for stem	n_{fall}^{stem}	month^{-1}	0.001	0.001	0.005	
… for root	n_{fall}^{root}	month^{-1}	0.003	0.007	0.008	
Rate limiting factor for maintenance respiration for leaf	Kr_b^{leaf}	month^{-1}	-6.0	-3.45	-2.95	-4.65
… for stem	Kr_b^{stem}	month^{-1}	-4.88	-5.15	-6.65	
… for root	Kr_b^{root}	month^{-1}	-8.2	-6.2	-3.2	

https://doi.org/10.5194/gmd-2024-158
Preprint. Discussion started: 25 September 2024

Table 4: Synthetic below-ground target values for the black spruce forest site used participated in the parameter calibration process

Name	Parameters	Unit	Value
Rate of microbial N uptake	n_{micb}^{up}	gg^{-1}	0.4495
Rate limiting factor of litter decomposition	kdc_{rawC}	$month^{-1}$	0.634
Rate limiting factor of active pool decomposition	kdc_{soma}	$month^{-1}$	0.54
Rate limiting factor of physically resistant pool decomposition	kdc_{sompr}	$month^{-1}$	0.002
Rate limiting factor of chemically resistant pool decomposition	kdc_{somcr}	$month^{-1}$	0.00007

3 Results

3.1 Vegetation Targets

Depending on the range of parameter variance, our analysis revealed varying levels of accuracy between known synthetic parameters a those determined using the MADS search approach. In general, the variance between calibrated and synthetic values grew higher with a higher degree of variance (Figure S2-S5). The averaged RMSE values for all four PFTs showed similar increases (Figure 3) with an exception for $C_{stem}(c_{fall})$ deciduous shrubs, which made the RMSE score for the 10% variance higher than the 20% variance (Figure 3a and 3b). That is why we introduced the RE metric, which shows that the departure between synthetic and calibrated parameters increases with increasing perturbation and is the smallest for the 10% variance (Figure 4a).

3.2 Vegetation Parameters

The RMSE for parameters was highest for Kr_b^{root} in the evergreen tree PFT (Figure 4). Overall, Kr_bs and n_{max} parameters exhibited the worst recovery compared to other parameters based on the RMSE metric. Conversely, REs were highest for c_{fall} deciduous shrubs and less for Kr_bs. The RE indicated that smaller parameter values, such as n_{fall}, deviated more significantly

https://doi.org/10.5194/gmd-2024-158
Preprint. Discussion started: 25 September 2024

from their synthetic values. Interestingly the RE score showed the same error range for 10% and 20% variance ranges, whereas RMSE showed that 10% variance has the smallest error.

3.3 Soil parameters

In general, the RMSE values for the sub-surface target parameters were relatively small but increased with a higher variance range (Figure 5). Notably, C_{deep} and $\sum\ C_{mineral}$ exhibited high RMSE values of 3.34 and 9.12, respectively, for the 10% variance range (Figure 5a). Despite this, the soil parameters for 10% variance showed the best match, with RMSE values less than 0.01. The RE for targets revealed increasing deviations from the synthetic parameter values for $\sum\ N_{avail}$. The RE for parameters indicated that n_{micb}^{up}, kdc_{rawC} and kdc_{soma} had higher deviations from their respective synthetic values for the 50% and 90% variance range, respectively.

https://doi.org/10.5194/gmd-2024-158
Preprint. Discussion started: 25 September 2024

Geoscientific Model Development
Discussions

Figure. 3. a), b), c), and d) are root mean square error (RMSE) metric and e), f), g), and h) are relative error (RE) metric for 10%, 20%, 50%, and 90% variance in the parameter range, correspondingly. Targets shown on y-axis, and plant functional types are on x-axis. The colorbar represents the RMSE and RE scores.

322
323

https://doi.org/10.5194/gmd-2024-158
Preprint. Discussion started: 25 September 2024

Geoscientific Model Development
Discussions
Open Access

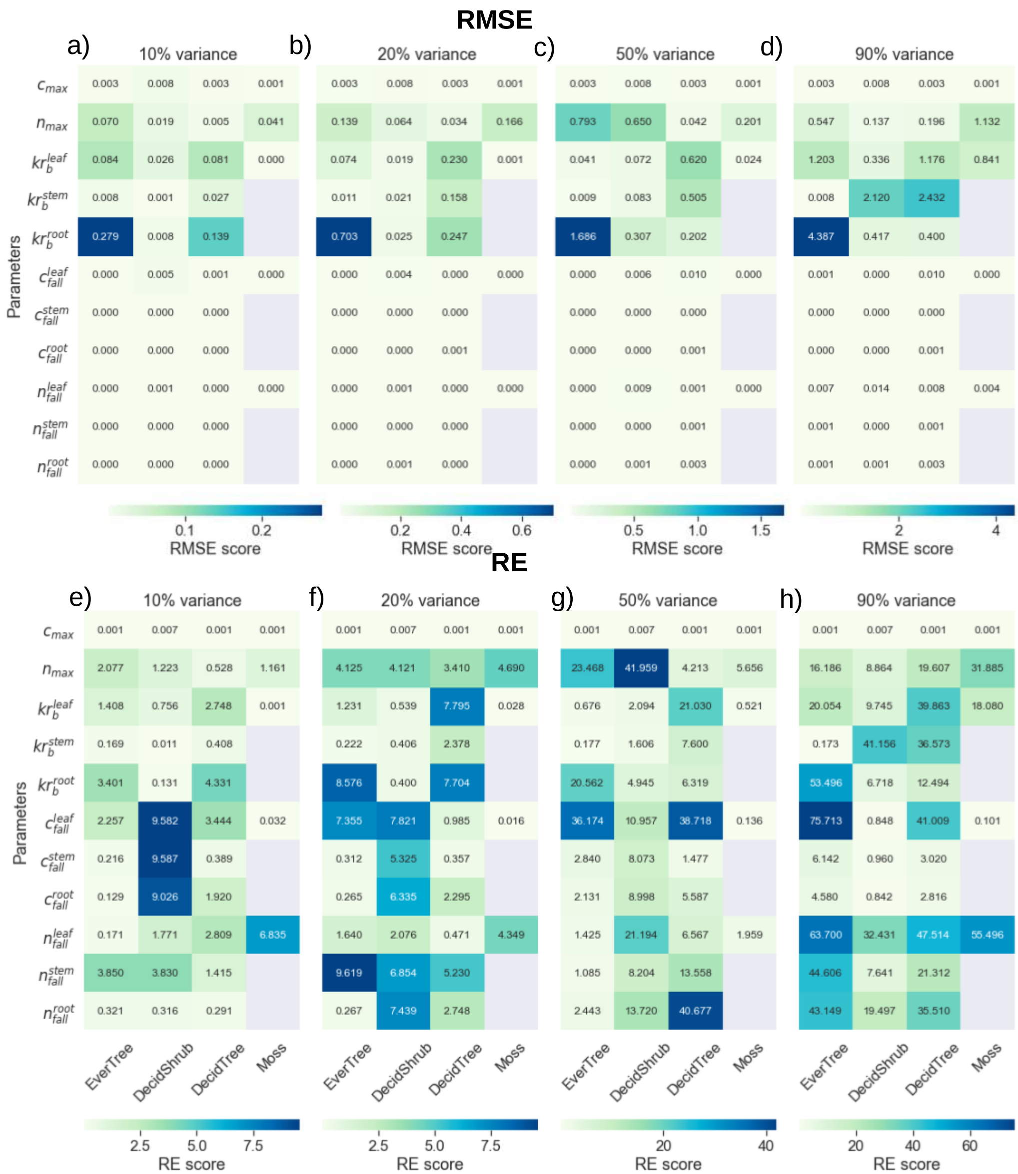

Figure 4. a), b), c), and d) are root mean square error (RMSE) metric and e), f), g), and h) are relative error (RE) metric for 10%, 20%, 50%, and 90% variance in the parameter range, correspondingly. DVM-DOS-TEM parameters shown on y-axis, and plant functional types are on x-axis. The colorbar represents the RMSE and RE scores

324

https://doi.org/10.5194/gmd-2024-158
Preprint. Discussion started: 25 September 2024

Geoscientific Model Development Discussions
Open Access
EGU

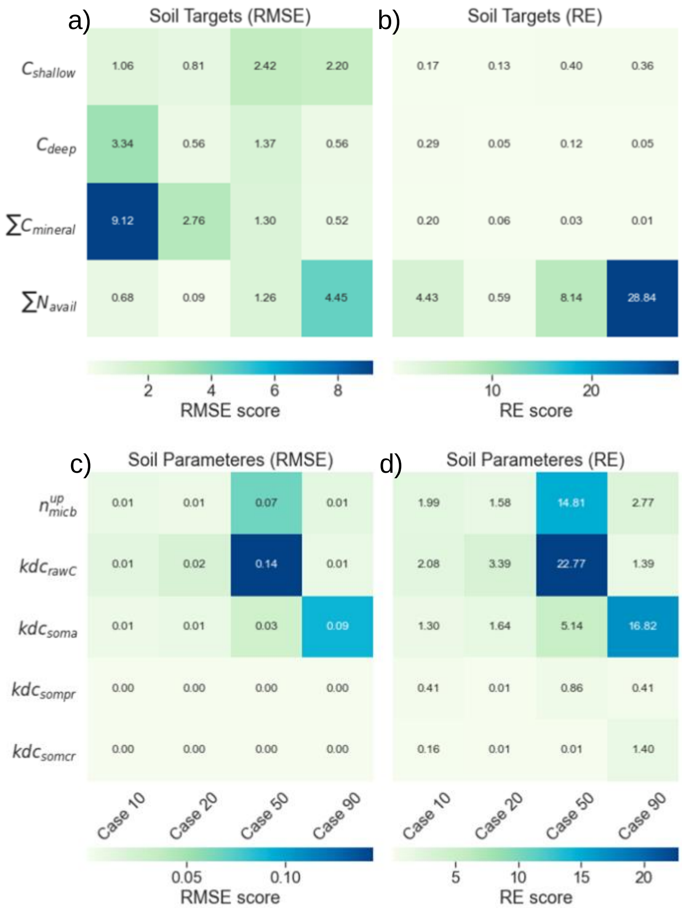

Figure 5. Comparison between calibrated and synthetic sub-surface target values (a) root mean square error (RMSE) and (b) relative error (RE) scores. Comparison between calibrated and synthetic sub-surface parameter values (a) root mean square error (RMSE) and (b) relative error (RE) scores for all range variances. The colorbar represents the RMSE and RE score.

4 Discussion

4.1 Importance of the initial guess

The importance of initial values, or the so-called initial guess, did not significantly impact our synthetic experiment because the perturbed parameter values were close enough to the true state. However, for non-synthetic calibrations, the initial state is crucial (Euskirchen et al., 2022; Yi et al., 2009). Applying calibration with parameter values far from the true values could

https://doi.org/10.5194/gmd-2024-158
Preprint. Discussion started: 25 September 2024

Geoscientific Model Development
Discussions

lead to non-convergence of the method and increased computation time. Therefore, when using real observations, starting with a good initial guess is essential. We developed parameter sensitivity methods to provide better estimates for the initial guess (Briones et al., 2024). The current experiment proves that MADS can accurately recover true parameter states well enough when the initial guess is well set.

4.2 Analysis of the recovery metrics

The mean parameter values calculated from the five best-matched MADS value predictions align closely with the synthetic parameter values, demonstrating the method's efficacy. The calculated REs for parameters indicate that the relative distance between the calibrated and the synthetic values increases with a higher parameter variance range, except RE for soil targets (Figure 5b). In many cases the RMSE for calibrated target values showed a higher distance for 10% variance range than for 20% variance range (Figure 3a and 3b). In addition, the RMSEs for 10% variance range for the soil targets were higher than any other variance range (Figure 5a). The mixed results between 10% and 20% variance range as well as soil target high RMSE for 10% variance, could be attributed to the limited number of cases participated in each variance case. The total number of randomly perturbed initial guesses within the given variance range was 10. It is possible that increasing the total number of searches would yield a more consistent pattern of decreasing accuracy with increasing variance.

4.3 Parameter-target relationship and small parameter values

The method demonstrated robust recovery of c_{max} values, indicating that it performs best when there is a linear relationship between parameters and target values (Eq. S1). For parameters, which do not exhibit a linear relationship with their target values (e.g. Kr_b, Eq. S4), the calibrated parameters showed wider variance. Additionally, small parameter values, such as n_{fall}, corresponded to small range values, leading to insensitivity between n_{fall} and vegetation N. To address this, we applied a logarithmic transformation to these and to some other small values for soil C rates.

4.4 The impact of n_{max} on N uptake and NPP

Sensitivity between model parameters and targets is crucial for effective parameter calibration. We observed that the sensitivity between n_{max} and NPP was not strong (Eq. S2, Eq. S5), which led us to combine its calibration with the Kr_b parameter. Based on (Eq. S2), n_{max} directly influences N_{uptake}. An increase in n_{max} enhances N_{uptake}, thereby increasing the total N supply. Since NPP is proportional to N_{supply} and inversely proportional to $N_{required}$, a higher N supply can lead to a higher NPP, provided that other factors remain constant. Therefore, despite the initial observation of weak sensitivity, n_{max} could have a considerable impact on NPP due to its role in N_{uptake} and the overall N_{supply}. However, our target values for plant N uptake are poorly constrained due to a lack of sufficient observations. This underestimation of plant N uptake could account for the observed lack of sensitivity of NPP to n_{max}. This issue requires further investigation and currently underscores the importance of accurately calibrating n_{max} to ensure better simulation of ecosystem productivity.

https://doi.org/10.5194/gmd-2024-158
Preprint. Discussion started: 25 September 2024

4.5 The Calibration Workflow

The setup of the calibration workflow is important for achieving accurate parameter estimation in terrestrial ecosystem models, considering the model organization by hierarchical levels associated with feedback and turnover of the ecological processes represented. Our findings indicate that calibrating one or two parameter sets at a time, while keeping other parameters constant, is more effective than calibrating all parameters simultaneously. For example in the current workflow, we combined n_{max} and Kr_b (Figure 2 Step a), which was based on the low sensitivity of n_{max} to NPP. Combining multiple variables in one calibration step increases the compute time and could result in low match accuracy. On the other hand, sequential parameter calibration carries the risk of losing accuracy for parameters calibrated in previous steps. To mitigate this risk, we include targets from previous calibration steps in the current calibration step. For example, when optimizing for n_{fall}, we include targets for NPP, vegetation C, and vegetation N.

Calibrating one parameter at a time is advantageous not only computationally but also in preventing the occurrence of an underdetermined problem, which arise when the number of parameters exceeds the number of targets. Undetermined problems exhibit a lower rate of convergence due to the correlation between parameters and the sensitivity of multiple parameters to one or a few similar target values. The study by Jafarov et al., (2020) showed that overdetermined problems, i.e. higher and diverse number of target values, are more effective in recovering accurate parameter values.

4.6 Sensitivity of the Kr_b parameter to NPP and vegetation C

The Kr_b parameter exhibited higher sensitivity to both NPP and vegetation C compared to other parameters. Despite the overall good model fitness, the deviation from the synthetic values for Kr_b was higher. This was primarily due to Kr_b^{root} parameter for evergreen tree (Figure S2) persistently showed higher discrepancy. Its sensitivity can be explained by examining its role in the equations governing maintenance respiration (R_m Eq. S3). The relationship between biomass and maintenance respiration is non-linear; R_m increases as biomass increases, where Kr_b controls the intercept of this relationship (Tian et al., 1999). Since NPP is computed as a resultant of GPP and autotrophic respiration, including R_m, any alteration in Kr_b impacts NPP directly (Eq. S9). This sensitivity underscores the importance of accurately calibrating Kr_b to ensure the correct simulation of ecosystem productivity and C dynamics in the DVM-DOS-TEM.

4.7 Vegetation and Below-Ground C stocks equilibrium time

Since vegetation C and N is characterized by faster turnover than soil carbon dynamic, vegetation C and N stocks and fluxes equilibrate faster than soil C and N stocks and fluxes, we used a two-phase equilibration approach: 200 years for the vegetation and 2000 years for the soil. However, the C stocks achieved after 200 years of equilibration for vegetation might shift when the model is run for an additional 1800 years to equilibrate soil. To mitigate this issue, we developed equilibrium checks to ensure that the vegetation stocks remain stable and close to their equilibrium values throughout the extended simulation period required for soil stocks equilibration. These equilibrium checks help identify significant departures from the initial equilibrium values of vegetation C while allowing the model to run for a longer duration to achieve below-ground C equilibrium. This approach ensures the accuracy and stability of both vegetation and below-ground C stocks in long-term model simulations.

5. Conclusion

In this study, we showed that the developed MADS parameter calibration method for the DVM-DOS-TEM can effectively recover the synthetic parameter set, optimizing labor and time, and enhancing reproducibility of the calibration process. By implementing a structured workflow that calibrates one or two parameters at a time and including equilibrium checks the method ensured accurate parameter estimation even for high variance parameter range. The primary advantage of the semi-automated MADS calibration approach is its significant enhancement of repeatability and clear quantification of calibration performance. In contrast, manual calibration processes are often difficult to reproduce as it is impractical if not impossible, to record users continuous adjustments to parameters values until improved results were achieved. Additionally, appreciation of model improvement by the user is often subjective as running a statistical evaluation at each parameter adjustment would be too time consuming. In the approach demonstrated in this study, we introduced a calibration metric that provides a quantifiable measure of the overall quality of the calibration. This metric enhances reproducibility by allowing future users working on the same site to follow the established workflow and reliably reproduce the calibrated parameter and target values. The RMSE quantifies the average differences between calibrated and observed (synthetic) values, while the RE metric indicates deviations from the synthetic values.

In all calibration experiments, we utilized only ten randomly perturbed initial parameter sets within a specified variance range. Our results indicated that perturbation ranges of 10%-20% were equally effective in achieving optimal target/parameter calibration. However, increasing the number of random perturbations could potentially shift the statistics, favoring a 10% variance range. Based on our findings, we recommend maintaining a small parameter variance interval, as this approach is likely to provide a robust match with target values and ensure effective parameter calibration.

While the choice of the initial guess is crucial, its impact was mitigated in our study due to the design involving variance around synthetic parameter values. The developed method significantly reduces the labor and time required for calibrating DVM-DOS-TEM model parameters. However, it does not entirely replace the need for human intervention. Users still need to understand the specifics of the model and the relationship between parameters and targets, as well as conduct post-processing assessments of the fit. In future work, we will apply this method to data processed at multiple study sites to validate further and refine the calibration approach.

6. Data and model availability

The version of the model used in these simulations, along with the calibration scripts, auxiliary files (including plots presented in the paper), and corresponding output files, are available at the following link: https://doi.org/10.5281/zenodo.13772987.

7. Author contributions

EEJ designed and executed the experiment. HG supervised in experiment design. VV supervised with MADS model. RR, TC, and DT provided technical support on the DVM-DOS-TEM model. VB, AK, ALM, BM, C-CC, and JC tested calibration approach. TS technical support on scientific computing. All authors participated in manuscript writing and editing. SMN and BMR provided overall supervision and research funding.

8. Competing interests

The contact author has declared that none of the authors has any competing interests.

9. Disclaimer

Publisher's note: Copernicus Publications remains neutral with regard to jurisdictional claims in published maps and institutional affiliations.

10. Acknowledgments

This work was supported by the Quadrature Climate Foundation (grant number 01-21-000094) and catalyzed through the Audacious Project (Permafrost Pathways) to SMN and BMR.

11. References

Andresen, C. G., Lawrence, D. M., Wilson, C. J., McGuire, A. D., Koven, C., Schaefer, K., Jafarov, E., Peng, S., Chen, X., Gouttevin, I., Burke, E., Chadburn, S., Ji, D., Chen, G., Hayes, D., and Zhang, W.: Soil moisture and hydrology projections of the permafrost region – a model intercomparison, The Cryosphere, 14, 445–459, https://doi.org/10.5194/tc-14-445-2020, 2020.

Barajas-Solano, D. A., Wohlberg, B. E., Vesselinov, V. V., and Tartakovsky, D. M.: Linear functional minimization for inverse modeling, Water Resources Research, 51, 4516–4531, https://doi.org/10.1002/2014WR016179, 2015.

Beven, K. and Freer, J.: Equifinality, data assimilation, and uncertainty estimation in mechanistic modelling of complex environmental systems using the GLUE methodology, Journal of Hydrology, 249, 11–29, https://doi.org/10.1016/S0022-1694(01)00421-8, 2001.

Bloom, A. A., Exbrayat, J.-F., Van Der Velde, I. R., Feng, L., and Williams, M.: The decadal state of the terrestrial carbon cycle: Global retrievals of terrestrial carbon allocation, pools, and residence times, Proc. Natl. Acad. Sci. U.S.A., 113, 1285–1290, https://doi.org/10.1073/pnas.1515160113, 2016.

Briones, V., Jafarov, E. E., Genet, H., Rogers, B. M., Rutter, R. M., Carman, T. B., Clein, J., Euschkirchen, E. S., Schuur, E. A., Watts, J. D., and Natali, S. M.: Exploring the interplay between soil thermal and hydrological changes and their impact on carbon fluxes in permafrost ecosystems, Environ. Res. Lett., 19, 074003, https://doi.org/10.1088/1748-9326/ad50ed, 2024.

Brunetti, G., Šimunek, J., Wöhling, T., and Stumpp, C.: An in-depth analysis of Markov-Chain Monte Carlo ensemble samplers for inverse vadose zone modeling, Journal of Hydrology, 624, 129822, https://doi.org/10.1016/j.jhydrol.2023.129822, 2023.

Calef, M. P., David McGuire, A., Epstein, H. E., Scott Rupp, T., and Shugart, H. H.: Analysis of vegetation distribution in Interior Alaska and sensitivity to climate change using a logistic regression approach, Journal of Biogeography, 32, 863–878, https://doi.org/10.1111/j.1365-2699.2004.01185.x, 2005.

Castelletti, A., Galelli, S., Ratto, M., Soncini-Sessa, R., and Young, P. C.: A general framework for Dynamic Emulation Modelling in environmental problems, Environmental Modelling & Software, 34, 5–18, https://doi.org/10.1016/j.envsoft.2012.01.002, 2012.

Chapin, F. S. and Kedrowski, R. A.: Seasonal Changes in Nitrogen and Phosphorus Fractions and Autumn Retranslocation in Evergreen and Deciduous Taiga Trees, Ecology, 64, 376–391, https://doi.org/10.2307/1937083, 1983.

Dagon, K., Sanderson, B. M., Fisher, R. A., and Lawrence, D. M.: A machine learning approach to emulation and biophysical parameter estimation with the Community Land Model, version 5, Adv. Stat. Clim. Meteorol. Oceanogr., 6, 223–244, https://doi.org/10.5194/ascmo-6-223-2020, 2020.

Dietze, M. C., Fox, A., Beck-Johnson, L. M., Betancourt, J. L., Hooten, M. B., Jarnevich, C. S., Keitt, T. H., Kenney, M. A., Laney, C. M., Larsen, L. G., Loescher, H. W., Lunch, C. K., Pijanowski, B. C., Randerson, J. T., Read, E. K., Tredennick, A. T., Vargas, R., Weathers, K. C., and White, E. P.: Iterative near-term ecological forecasting: Needs, opportunities, and challenges, Proc. Natl. Acad. Sci. U.S.A., 115, 1424–1432, https://doi.org/10.1073/pnas.1710231115, 2018.

Efstratiadis, A. and Koutsoyiannis, D.: One decade of multi-objective calibration approaches in hydrological modelling: a review, Hydrological Sciences Journal, 55, 58–78, https://doi.org/10.1080/02626660903526292, 2010.

Euskirchen, E. S., McGUIRE, A. D., Kicklighter, D. W., Zhuang, Q., Clein, J. S., Dargaville, R. J., Dye, D. G., Kimball, J. S., McDONALD, K. C., Melillo, J. M., Romanovsky, V. E., and Smith, N. V.: Importance of recent shifts in soil thermal dynamics on growing season length, productivity, and carbon sequestration in terrestrial high-latitude ecosystems: HIGH-LATITUDE CLIMATE CHANGE INDICATORS, Global Change Biology, 12, 731–750, https://doi.org/10.1111/j.1365-2486.2006.01113.x, 2006.

Euskirchen, E. S., McGuire, A. D., Chapin, F. S., Yi, S., and Thompson, C. C.: Changes in vegetation in northern Alaska under scenarios of climate change, 2003–2100: implications for climate feedbacks, Ecological Applications, 19, 1022–1043, https://doi.org/10.1890/08-0806.1, 2009.

Euskirchen, E. S., Edgar, C. W., Turetsky, M. R., Waldrop, M. P., and Harden, J. W.: Differential response of carbon fluxes to climate in three peatland ecosystems that vary in the presence and stability of permafrost: Carbon fluxes and permafrost thaw, J. Geophys. Res. Biogeosci., 119, 1576–1595, https://doi.org/10.1002/2014JG002683, 2014.

Euskirchen, E. S., Serbin, S. P., Carman, T. B., Fraterrigo, J. M., Genet, H., Iversen, C. M., Salmon, V., and McGuire, A. D.: Assessing dynamic vegetation model parameter uncertainty across Alaskan arctic tundra plant communities, Ecological Applications, 32, https://doi.org/10.1002/eap.2499, 2022.

https://doi.org/10.5194/gmd-2024-158
Preprint. Discussion started: 25 September 2024

Geoscientific Model Development Discussions

Fer, I., Kelly, R., Moorcroft, P. R., Richardson, A. D., Cowdery, E. M., and Dietze, M. C.: Linking big models to big data: efficient ecosystem model calibration through Bayesian model emulation, Biogeosciences, 15, 5801–5830, https://doi.org/10.5194/bg-15-5801-2018, 2018.

Forrester, A. I. J., Bressloff, N. W., and Keane, A. J.: Optimization using surrogate models and partially converged computational fluid dynamics simulations, Proc. R. Soc. A., 462, 2177–2204, https://doi.org/10.1098/rspa.2006.1679, 2006.

Fox, A. M., Hoar, T. J., Anderson, J. L., Arellano, A. F., Smith, W. K., Litvak, M. E., MacBean, N., Schimel, D. S., and Moore, D. J. P.: Evaluation of a Data Assimilation System for Land Surface Models Using CLM4.5, J Adv Model Earth Syst, 10, 2471–2494, https://doi.org/10.1029/2018MS001362, 2018.

Genet, H., McGuire, A. D., Barrett, K., Breen, A., Euskirchen, E. S., Johnstone, J. F., Kasischke, E. S., Melvin, A. M., Bennett, A., Mack, M. C., Rupp, T. S., Schuur, A. E. G., Turetsky, M. R., and Yuan, F.: Modeling the effects of fire severity and climate warming on active layer thickness and soil carbon storage of black spruce forests across the landscape in interior Alaska, Environ. Res. Lett., 8, 045016, https://doi.org/10.1088/1748-9326/8/4/045016, 2013.

Genet, H., He, Y., Lyu, Z., McGuire, A. D., Zhuang, Q., Clein, J., D'Amore, D., Bennett, A., Breen, A., Biles, F., Euskirchen, E. S., Johnson, K., Kurkowski, T., (Kushch) Schroder, S., Pastick, N., Rupp, T. S., Wylie, B., Zhang, Y., Zhou, X., and Zhu, Z.: The role of driving factors in historical and projected carbon dynamics of upland ecosystems in Alaska, Ecol Appl, 28, 5–27, https://doi.org/10.1002/eap.1641, 2018.

Hansen, P. C.: Rank-Deficient and Discrete Ill-Posed Problems: Numerical Aspects of Linear Inversion, Society for Industrial and Applied Mathematics, https://doi.org/10.1137/1.9780898719697, 1998.

Harp, D. R., Atchley, A. L., Painter, S. L., Coon, E. T., Wilson, C. J., Romanovsky, V. E., and Rowland, J. C.: Effect of soil property uncertainties on permafrost thaw projections: a calibration-constrained analysis, The Cryosphere, 10, 341–358, https://doi.org/10.5194/tc-10-341-2016, 2016.

Harris, I., Jones, P. D., Osborn, T. J., and Lister, D. H.: Updated high-resolution grids of monthly climatic observations - the CRU TS3.10 Dataset: UPDATED HIGH-RESOLUTION GRIDS OF MONTHLY CLIMATIC OBSERVATIONS, Int. J. Climatol., 34, 623–642, https://doi.org/10.1002/joc.3711, 2014.

Hugelius, G., Strauss, J., Zubrzycki, S., Harden, J. W., Schuur, E. A. G., Ping, C.-L., Schirrmeister, L., Grosse, G., Michaelson, G. J., Koven, C. D., O'Donnell, J. A., Elberling, B., Mishra, U., Camill, P., Yu, Z., Palmtag, J., and Kuhry, P.: Estimated stocks of circumpolar permafrost carbon with quantified uncertainty ranges and identified data gaps, Biogeosciences, 11, 6573–6593, https://doi.org/10.5194/bg-11-6573-2014, 2014.

Jafarov, E. E., Romanovsky, V. E., Genet, H., McGuire, A. D., and Marchenko, S. S.: The effects of fire on the thermal stability of permafrost in lowland and upland black spruce forests of interior Alaska in a changing climate, Environ. Res. Lett., 8, 035030, https://doi.org/10.1088/1748-9326/8/3/035030, 2013.

Jafarov, E. E., Nicolsky, D. J., Romanovsky, V. E., Walsh, J. E., Panda, S. K., and Serreze, M. C.: The effect of snow: How to better model ground surface temperatures, Cold Regions Science and Technology, 102, 63–77, https://doi.org/10.1016/j.coldregions.2014.02.007, 2014.

Jafarov, E. E., Harp, D. R., Coon, E. T., Dafflon, B., Tran, A. P., Atchley, A. L., Lin, Y., and Wilson, C. J.: Estimation of subsurface porosities and thermal conductivities of polygonal tundra by coupled inversion of electrical resistivity, temperature, and moisture content data, The Cryosphere, 14, 77–91, https://doi.org/10.5194/tc-14-77-2020, 2020.

https://doi.org/10.5194/gmd-2024-158
Preprint. Discussion started: 25 September 2024

Jean, M., Melvin, A. M., Mack, M. C., and Johnstone, J. F.: Broadleaf Litter Controls Feather Moss Growth in Black Spruce and Birch Forests of Interior Alaska, Ecosystems, 23, 18–33, https://doi.org/10.1007/s10021-019-00384-8, 2020.

Kelly, R., Chipman, M. L., Higuera, P. E., Stefanova, I., Brubaker, L. B., and Hu, F. S.: Recent burning of boreal forests exceeds fire regime limits of the past 10,000 years, Proc. Natl. Acad. Sci. U.S.A., 110, 13055–13060, https://doi.org/10.1073/pnas.1305069110, 2013.

Koziel, S., Ciaurri, D. E., and Leifsson, L.: Surrogate-Based Methods, in: Computational Optimization, Methods and Algorithms, vol. 356, edited by: Koziel, S. and Yang, X.-S., Springer Berlin Heidelberg, Berlin, Heidelberg, 33–59, https://doi.org/10.1007/978-3-642-20859-1_3, 2011.

Lara, M. J., Genet, H., McGuire, A. D., Euskirchen, E. S., Zhang, Y., Brown, D. R. N., Jorgenson, M. T., Romanovsky, V., Breen, A., and Bolton, W. R.: Thermokarst rates intensify due to climate change and forest fragmentation in an Alaskan boreal forest lowland, Global Change Biology, 22, 816–829, https://doi.org/10.1111/gcb.13124, 2016.

Levenberg, K.: A METHOD FOR THE SOLUTION OF CERTAIN NON-LINEAR PROBLEMS IN LEAST SQUARES, Quarterly of Applied Mathematics, 2, 164–168, 1944.

Lin, Y., O'Malley, D., and Vesselinov, V. V.: A computationally efficient parallel L evenberg- M arquardt algorithm for highly parameterized inverse model analyses, Water Resources Research, 52, 6948–6977, https://doi.org/10.1002/2016WR019028, 2016.

Linde, N., Renard, P., Mukerji, T., and Caers, J.: Geological realism in hydrogeological and geophysical inverse modeling: A review, Advances in Water Resources, 86, 86–101, https://doi.org/10.1016/j.advwatres.2015.09.019, 2015.

Ling, X.-L., Fu, C.-B., Yang, Z.-L., and Guo, W.-D.: Comparison of different sequential assimilation algorithms for satellite-derived leaf area index using the Data Assimilation Research Testbed (version Lanai), Geosci. Model Dev., 12, 3119–3133, https://doi.org/10.5194/gmd-12-3119-2019, 2019.

Luo, Y., Ahlström, A., Allison, S. D., Batjes, N. H., Brovkin, V., Carvalhais, N., Chappell, A., Ciais, P., Davidson, E. A., Finzi, A., Georgiou, K., Guenet, B., Hararuk, O., Harden, J. W., He, Y., Hopkins, F., Jiang, L., Koven, C., Jackson, R. B., Jones, C. D., Lara, M. J., Liang, J., McGuire, A. D., Parton, W., Peng, C., Randerson, J. T., Salazar, A., Sierra, C. A., Smith, M. J., Tian, H., Todd-Brown, K. E. O., Torn, M., Van Groenigen, K. J., Wang, Y. P., West, T. O., Wei, Y., Wieder, W. R., Xia, J., Xu, X., Xu, X., and Zhou, T.: Toward more realistic projections of soil carbon dynamics by Earth system models, Global Biogeochemical Cycles, 30, 40–56, https://doi.org/10.1002/2015GB005239, 2016.

MacBean, N., Peylin, P., Chevallier, F., Scholze, M., and Schürmann, G.: Consistent assimilation of multiple data streams in a carbon cycle dataassimilation system, Geosci. Model Dev., 9, 3569–3588, https://doi.org/10.5194/gmd-9-3569-2016, 2016.

Marquardt, D. W.: An Algorithm for Least-Squares Estimation of Nonlinear Parameters, Journal of the Society for Industrial and Applied Mathematics, 11, 431–441, 1963.

McGuire, A. D., Koven, C., Lawrence, D. M., Clein, J. S., Xia, J., Beer, C., Burke, E., Chen, G., Chen, X., Delire, C., Jafarov, E., MacDougall, A. H., Marchenko, S., Nicolsky, D., Peng, S., Rinke, A., Saito, K., Zhang, W., Alkama, R., Bohn, T. J., Ciais, P., Decharme, B., Ekici, A., Gouttevin, I., Hajima, T., Hayes, D. J., Ji, D., Krinner, G., Lettenmaier, D. P., Luo, Y., Miller, P. A., Moore, J. C., Romanovsky, V., Schädel, C., Schaefer, K., Schuur, E. A. G., Smith, B., Sueyoshi, T., and Zhuang, Q.: Variability in the sensitivity among model simulations of permafrost and carbon dynamics in the permafrost region between 1960 and 2009: MODELING PERMAFROST CARBON DYNAMICS, Global Biogeochem. Cycles, 30, 1015–1037, https://doi.org/10.1002/2016GB005405, 2016.

https://doi.org/10.5194/gmd-2024-158
Preprint. Discussion started: 25 September 2024

Geoscientific Model Development Discussions

McGuire, A. D., Lawrence, D. M., Koven, C., Clein, J. S., Burke, E., Chen, G., Jafarov, E., MacDougall, A. H., Marchenko, S., Nicolsky, D., Peng, S., Rinke, A., Ciais, P., Gouttevin, I., Hayes, D. J., Ji, D., Krinner, G., Moore, J. C., Romanovsky, V., Schädel, C., Schaefer, K., Schuur, E. A. G., and Zhuang, Q.: Dependence of the evolution of carbon dynamics in the northern permafrost region on the trajectory of climate change, Proc Natl Acad Sci USA, 115, 3882–3887, https://doi.org/10.1073/pnas.1719903115, 2018.

Melvin, A. M., Mack, M. C., Johnstone, J. F., David McGuire, A., Genet, H., and Schuur, E. A. G.: Differences in Ecosystem Carbon Distribution and Nutrient Cycling Linked to Forest Tree Species Composition in a Mid-Successional Boreal Forest, Ecosystems, 18, 1472–1488, https://doi.org/10.1007/s10021-015-9912-7, 2015.

Natali, S. M., Holdren, J. P., Rogers, B. M., Treharne, R., Duffy, P. B., Pomerance, R., and MacDonald, E.: Permafrost carbon feedbacks threaten global climate goals, Proc. Natl. Acad. Sci. U.S.A., 118, e2100163118, https://doi.org/10.1073/pnas.2100163118, 2021.

Nicolsky, D. J., Romanovsky, V. E., and Tipenko, G. S.: Using in-situ temperature measurements to estimate saturated soil thermal properties by solving a sequence of optimization problems, The Cryosphere, 1, 41–58, https://doi.org/10.5194/tc-1-41-2007, 2007.

Nicolsky, D. J., Romanovsky, V. E., and Panteleev, G. G.: Estimation of soil thermal properties using in-situ temperature measurements in the active layer and permafrost, Cold Regions Science and Technology, 55, 120–129, https://doi.org/10.1016/j.coldregions.2008.03.003, 2009.

O'Malley, D. and Vesselinov, V. V.: Bayesian-information-gap decision theory with an application to CO $_2$ sequestration: BAYESIAN-INFORMATION-GAP DECISION THEORY, Water Resour. Res., 51, 7080–7089, https://doi.org/10.1002/2015WR017413, 2015.

Pastick, N. J., Duffy, P., Genet, H., Rupp, T. S., Wylie, B. K., Johnson, K. D., Jorgenson, M. T., Bliss, N., McGuire, A. D., Jafarov, E. E., and Knight, J. F.: Historical and projected trends in landscape drivers affecting carbon dynamics in Alaska, Ecological Applications, 27, 1383–1402, https://doi.org/10.1002/eap.1538, 2017.

Peylin, P., Bacour, C., MacBean, N., Leonard, S., Rayner, P., Kuppel, S., Koffi, E., Kane, A., Maignan, F., Chevallier, F., Ciais, P., and Prunet, P.: A new stepwise carbon cycle data assimilation system using multiple data streams to constrain the simulated land surface carbon cycle, Geosci. Model Dev., 9, 3321–3346, https://doi.org/10.5194/gmd-9-3321-2016, 2016.

Pujol, J.: The solution of nonlinear inverse problems and the Levenberg-Marquardt method, GEOPHYSICS, 72, W1–W16, https://doi.org/10.1190/1.2732552, 2007.

Queipo, N. V., Haftka, R. T., Shyy, W., Goel, T., Vaidyanathan, R., and Kevin Tucker, P.: Surrogate-based analysis and optimization, Progress in Aerospace Sciences, 41, 1–28, https://doi.org/10.1016/j.paerosci.2005.02.001, 2005.

Razavi, S., Tolson, B. A., and Burn, D. H.: Review of surrogate modeling in water resources, Water Resources Research, 48, 2011WR011527, https://doi.org/10.1029/2011WR011527, 2012.

Regis, R. G. and Shoemaker, C. A.: A Stochastic Radial Basis Function Method for the Global Optimization of Expensive Functions, INFORMS Journal on Computing, 19, 497–509, https://doi.org/10.1287/ijoc.1060.0182, 2007.

Reichstein, M., Camps-Valls, G., Stevens, B., Jung, M., Denzler, J., Carvalhais, N., and Prabhat: Deep learning and process understanding for data-driven Earth system science, Nature, 566, 195–204, https://doi.org/10.1038/s41586-019-0912-1, 2019.

Ruess, R. W., Cleve, K. V., Yarie, J., and Viereck, L. A.: Contributions of fine root production and turnover to the carbon and nitrogen cycling in taiga forests of the Alaskan interior, Can. J. For. Res., 26, 1326–1336, https://doi.org/10.1139/x26-148, 1996.

Rykiel, E. J.: Testing ecological models: the meaning of validation, Ecological Modelling, 90, 229–244, https://doi.org/10.1016/0304-3800(95)00152-2, 1996.

Schädel, C., Rogers, B. M., Lawrence, D. M., Koven, C. D., Brovkin, V., Burke, E. J., Genet, H., Huntzinger, D. N., Jafarov, E., McGuire, A. D., Riley, W. J., and Natali, S. M.: Earth system models must include permafrost carbon processes, Nat. Clim. Chang., https://doi.org/10.1038/s41558-023-01909-9, 2024.

Scholze, M., Kaminski, T., Knorr, W., Blessing, S., Vossbeck, M., Grant, J. P., and Scipal, K.: Simultaneous assimilation of SMOS soil moisture and atmospheric CO2 in-situ observations to constrain the global terrestrial carbon cycle, Remote Sensing of Environment, 180, 334–345, https://doi.org/10.1016/j.rse.2016.02.058, 2016.

Schürmann, G. J., Kaminski, T., Köstler, C., Carvalhais, N., Voßbeck, M., Kattge, J., Giering, R., Rödenbeck, C., Heimann, M., and Zaehle, S.: Constraining a land-surface model with multiple observations by application of the MPI-Carbon Cycle Data Assimilation System V1.0, Geosci. Model Dev., 9, 2999–3026, https://doi.org/10.5194/gmd-9-2999-2016, 2016.

Schuur, E. A. G., Abbott, B. W., Commane, R., Ernakovich, J., Euskirchen, E., Hugelius, G., Grosse, G., Jones, M., Koven, C., Leshyk, V., Lawrence, D., Loranty, M. M., Mauritz, M., Olefeldt, D., Natali, S., Rodenhizer, H., Salmon, V., Schädel, C., Strauss, J., Treat, C., and Turetsky, M.: Permafrost and Climate Change: Carbon Cycle Feedbacks From the Warming Arctic, Annu. Rev. Environ. Resour., 47, 343–371, https://doi.org/10.1146/annurev-environ-012220-011847, 2022.

Shaver, G. R. and Chapin, F. S.: Long-term responses to factorial, NPK fertilizer treatment by Alaskan wet and moist tundra sedge species, Ecography, 18, 259–275, https://doi.org/10.1111/j.1600-0587.1995.tb00129.x, 1995.

Tian, H., Melillo, J. M., Kicklighter, D. W., McGuire, A. D., and Helfrich, J.: The sensitivity of terrestrial carbon storage to historical climate variability and atmospheric CO_2 in the United States, Tellus B: Chemical and Physical Meteorology, 51, 414, https://doi.org/10.3402/tellusb.v51i2.16318, 1999.

Tran, A. P., Dafflon, B., and Hubbard, S. S.: Coupled land surface–subsurface hydrogeophysical inverse modeling to estimate soil organic carbon content and explore associated hydrological and thermal dynamics in the Arctic tundra, The Cryosphere, 11, 2089–2109, https://doi.org/10.5194/tc-11-2089-2017, 2017.

Treharne, R., Rogers, B. M., Gasser, T., MacDonald, E., and Natali, S.: Identifying Barriers to Estimating Carbon Release From Interacting Feedbacks in a Warming Arctic, Front. Clim., 3, 716464, https://doi.org/10.3389/fclim.2021.716464, 2022.

Vesselinov V.V.: MADS: Model Analysis and Decision Support in Julia, https://github.com/madsjulia/Mads.jl, 2022.

Wutzler, T. and Carvalhais, N.: Balancing multiple constraints in model-data integration: Weights and the parameter block approach, JGR Biogeosciences, 119, 2112–2129, https://doi.org/10.1002/2014JG002650, 2014.

Xu, T., Valocchi, A. J., Ye, M., Liang, F., and Lin, Y.: Bayesian calibration of groundwater models with input data uncertainty, Water Resources Research, 53, 3224–3245, https://doi.org/10.1002/2016WR019512, 2017.

Yi, S., McGuire, A. D., Harden, J., Kasischke, E., Manies, K., Hinzman, L., Liljedahl, A., Randerson, J., Liu, H., Romanovsky, V., Marchenko, S., and Kim, Y.: Interactions between soil thermal and hydrological dynamics in the response of Alaska ecosystems to fire disturbance: SOIL THERMAL AND HYDROLOGICAL DYNAMICS, J. Geophys. Res., 114, n/a-n/a, https://doi.org/10.1029/2008JG000841, 2009.

Yi, S., McGuire, A. D., Kasischke, E., Harden, J., Manies, K., Mack, M., and Turetsky, M.: A dynamic organic soil biogeochemical model for simulating the effects of wildfire on soil environmental conditions and carbon dynamics of black spruce forests, J. Geophys. Res., 115, G04015, https://doi.org/10.1029/2010JG001302, 2010.

Zhuang, Q., McGuire, A. D., O'Neill, K. P., Harden, J. W., Romanovsky, V. E., and Yarie, J.: Modeling soil thermal and carbon dynamics of a fire chronosequence in interior Alaska, J. Geophys. Res., 108, 8147, https://doi.org/10.1029/2001JD001244, 2002.